

Contents lists available at ScienceDirect

Acta Materialia

journal homepage: www.elsevier.com/locate/actamat





Topological vortex induced large recoverable electrostrain with high temperature-stability in ferroelectric nano-dots

Xiaoqin Ke^a, Dong Wang^{a,*}, Sen Yang^a, Xiaobing Ren^b, Yunzhi Wang^c

- a School of Physics, MOE Key Laboratory for Nonequilibrium Synthesis and Modulation of Condensed Matter, Frontier Institute of Science and Technology, Xi'an Jiaotong University, Xi'an 710049, China
- ^b Ferroic Physics Group, National Institute for Materials Science, Tsukuba, Ibaraki 305-0047, Japan
- ^c Department of Materials Science and Engineering, The Ohio State University, Columbus 43210, USA

ARTICLE INFO

Keywords:
Ferroelectrics
Phase field
Topological vortex
Nano dots
Electrostrain

ABSTRACT

Here we report by phase field simulations that in ferroelectric nanodots the single domain generated from the vortex under external electric field will transform back to the vortex structure after removal of the field, which could offer large recoverable electrostrain during the process. Moreover, it is found that the recoverable electrostrain maintains a large value and could exist over a wide temperature range. The good recoverability of the vortex structure and electrostrain in the ferroelectric nanodots is found to be mainly ascribed to the dipole-dipole interaction energy and the elastic interaction energy in the system. This work may shed light on the development of miniaturized actuators in Micro-Electro-Mechanical System (MEMS) or Nano-Electromechanical System (NEMS).

1. Introduction

Ferroelectric materials normally exhibit multi-domain structures at bulk and topological structures such as vortices and skyrmions when their size goes to nanometer level as a result of the interplay among electrostatic energy, elastic energy and gradient energy [1-3]. The topological vortex has attracted intensive attention during the past two decades due to both its intriguing physics and emergent functionalities that can find applications in ultrahigh density data storage devices [4-9].

Upon applying a large enough homogeneous external electric field, the polarizations in both the multi-domain structure of bulk ferroelectrics and the vortex structure of nano ferroelectrics would align to the direction of external field and form a single domain [10,11]. Correspondingly, large electrostrain could be generated during the transformation from multidomain/vortex to single-domain structure as a result of the strong coupling between polarization and strain in ferroelectrics. Normally the single-domain structure generated from multi-domain structure under external electric field at bulk ferroelectrics would largely keep the single-domain state and not go back to the initial multi-domain structure after the removal of the field due to the usually large energy barrier between different domain variants [10,12]. The irreversibility of the multidomain to single-domain transformation

in conventional bulk ferroelectrics makes the large electrostrain obtained during the multidomain to single-domain transformation irrecoverable and thus greatly limits its application on actuators [12]. Although there are ways to bring the single-domain state back to multi-domain state upon removal of the electric field for bulk ferroelectrics, e.g., by introducing large local electric fields through doping a large number of point defects in ferroelectrics (i.e., relaxors) [13–15], the recoverable electrostrain in relaxors is obtained at the expense of sacrificing the magnitude of the electrostrain, not to mention its inferior temperature stability [15,16]. It is thus important to know whether the single-domain structure generated from vortex at nanoscale ferroelectrics under homogeneous electric field would go back to the initial vortex structure or not upon the removal of the electric field, which determines whether the electrostrain obtained during the vortex to single-domain transformation in nano ferroelectrics is recoverable or not and in turn determines whether or not nanosized ferroelectrics could be utilized as nano-actuators in Micro-Electro-Mechanical System (MEMS) or Nano-Electromechanical System (NEMS) [17].

There are a series of theoretical works devoted to studying the vortex to single-domain structure transformation, by varying parameters such as electric fields, mechanical fields, compositions and the screening conditions [11,18–22]. Although it has been mentioned in Ref. [20] that the single-domain structure obtained by applying a homogeneous

E-mail address: wang_dong1223@xjtu.edu.cn (D. Wang).

 $^{^{\}ast}$ Corresponding author.

electric field could revert back to the initial vortex structure upon removing the field at poor screening conditions, it is not the focus of Ref. [20] and thus the reversible transformation between single-domain and vortex structure under homogeneous electric field has not been systematically explored, especially how and why the single-domain structure reverts back to the vortex structure upon removal of electric field. More importantly, how the reversible transformation would affect the electrostrain property of ferroelectrics at nanoscale is unclear.

Here in this work we design a BaTiO₃ dot embedded in a nonferroelectric matrix and study the polarization hysteresis and electrostrain properties of these composite materials through phase field simulations. We find that as the dot size gradually decreases to nanometer level, the domain structure changes from multi-domain structure to polarization vortex structure. Interestingly, it has been found that the vortex structure in the confined ferroelectric nanodots could recover itself fully at zero electric field from the single-domain state obtained at large homogeneous electric fields due to the restoring force provided mainly by the dipole-dipole interaction energy and the elastic interaction energy. Correspondingly, the electrostrain is fully recoverable and the large recoverable electrostrain can be maintained over a wide temperature range. This work may shed light on the development of miniaturized actuators in MEMS and NEMS.

2. Phase field models

The total free energy F of the model system includes Landau free energy, F_{Landau} , the gradient energy, F_{grad} , the elastic strain energy, F_{elas} , the electrostatic energy, F_{elec} [23,24]:

$$F = F_{\text{Landau}} + F_{\text{grad}} + F_{\text{elas}} + F_{\text{elec}} = \int_{V} (f_{\text{Landau}} + f_{\text{grad}} + f_{\text{elas}} + f_{\text{elec}}) dV, \tag{1}$$

in which f_{Landau} , f_{grad} , f_{elas} , f_{elec} are the corresponding energy density and V is the volume of the system. The Landau free energy density f_{Landau} can be written in terms of P (P_1, P_2, P_3) as:

$$f_{\text{Landau}} = A_1 \sum_{i=1,2,3} P_i^2 + A_2 \left(\sum_{i=1,2,3} P_i^2 \right)^2 + A_3 \left(\sum_{i=1,2,3} P_i^2 \right)^3 + A_{12} \left(\sum_{i,j=1,2,3}^{i \neq j} P_i^2 P_j^2 \right) + A_{13} \sum_{i,j=1,2,3}^{i \neq j} P_i^2 P_j^4 + A_{14} \left(P_1^2 P_2^2 P_3^2 \right)$$
(2)

where A_1 , A_2 , A_3 , A_{12} , A_{13} , and A_{14} are the Landau coefficients and depend on T (temperature). The gradient energy density $f_{\rm grad}$ is written in terms of P as follows: $f_{\rm grad} = \frac{1}{2} \rho \sum_{i,j=1,2,3} (P_{i,j})^2$, where β is the gradient energy coefficient. The elastic energy density $f_{\rm elas}$ is calculated by $f_{\rm elas} = \frac{1}{2} C_{ijkl} e_{ij} e_{kl} = \frac{1}{2} C_{ijkl} (\varepsilon_{ij} - \varepsilon_{ij}^0) (\varepsilon_{kl} - \varepsilon_{kl}^0)$, where C_{ijkl} is the elastic constant, $e_{ij,\epsilon_{ij}}, \varepsilon_{ij}^0$ is the elastic strain, total strain, and spontaneous strain, respectively. The spontaneous strain is obtained from the polarization P by $\varepsilon_{ij}^0 = Q_{ijkl} P_k P_l$, where Q_{ijkl} is the electrostrictive coefficient. The electrostatic energy density is calculated by $f_{\rm elec} = \sum_{i=1,2,3} - \frac{1}{2} E_i P_i - \frac{1}{2} E_{i,{\rm depol}} \overline{P_i} - E_{i,{\rm app}} P_i$, where E_i denotes the inhomogeneous electric field due to the dipole-dipole interactions, $E_{i,{\rm depol}}$ denotes the average depolarization field due to the surface charge, $\overline{P_i}$ denotes the average polarization, $E_{i,{\rm app}}$ denotes the applied external electric field. The temporal dependence of the spontaneous polarization can be obtained by solving the time-dependent Ginzburg-Landau (TDGL) function given by:

$$\frac{\partial P_i}{\partial t} = -M \frac{\delta F}{\delta P_i} + \zeta, i = 1, 2, 3 \tag{3}$$

where M is the mobility coefficient and t is the time, $\zeta = \sqrt{2k_BTM/(l_0^3\Delta t)}\rho$ represents the thermal fluctuation and is described by the random number ρ in simulations [25].

The parameters used in the simulations are the same as those used in Ref. [26]. In the simulations, BaTiO $_3$ ferroelectric dots with different diameters (D=400 nm, 200 nm, 80 nm and 40 nm) are embedded in a paraelectric non-transforming matrix (e.g., polymer) with constraint elastic boundary. It is assumed that the interface between the ferroelectric nanodots and the matrix is charge-free. Note that changing the electrical boundary condition would dramatically affect the polarization structure formed in nano ferroelectrics, as intensively discussed in existing literature [27–29] and we do not discuss this effect in our simulations.

3. Results and discussions

3.1. Formation of polar vortex structure at ferroelectric nanodots

Fig. 1 shows the domain structure of ferroelectric dots with different diameters (*D*) at 40 °C. It is seen that at large sizes (D=400 nm, 200 nm, 80 nm), the dot exhibits a multidomain state which is similar to bulk ferroelectric materials. Ample 90° and 180° domain boundaries are found in these domain structures. When the size of nanodots is reduced to a certain level (such as D=40 nm), the dot exhibits a vortex-like domain structure with four 90° domain boundaries and one intersecting point of the four boundaries (i.e., the center point). Such vortex-like structure at reduced physical dimensions is consistent with previous experimental observations [30–32], first-principle simulations [4,33] as well as phase field simulations [34,35]. The formation of the vortex structure is due to the delicate balance between electrostatic energy, elastic energy, and polarization gradient energy [5].

3.2. Recoverable electrostrain obtained in ferroelectric nanodots with polar vortex structure and its temperature stability

The polarization (*P*)-electric field (*E*) loop and strain (*S*)-*E* loop of these ferroelectric dots with different sizes at T=60 °C and T=20 °C are calculated and the results are shown in Fig. 2. The D=400 nm dot with initial multidomain structure displays conventional polarization-field loops and butterfly-shaped strain-field loops at both temperatures. With the reduction of the dot size, it is seen that the *P*-*E* loop becomes pinched and the *S*-*E* loop becomes more and more recoverable. It is illustrated that the D=40 nm dot with initial vortex structure shown in Fig. 1 displays double hysteresis loops and fully recoverable electrostrain at both temperatures. Such results suggest that the ferroelectric vortex structure in ferroelectric nanodots could be fully recoverable upon removal of external electric field once it is transformed to single-domain state by external field, which is consistent with experimental observations reported in Ref. [36].

The strain-electric field loops of D=40 nm nanodot at several different temperatures between 80 and $\cdot 20^{\circ}\text{C}$ are calculated and given in Fig. 3. It is illustrated that the electrostrain is fully recoverable for all temperatures between 80 and $\cdot 20^{\circ}\text{C}$ for D=40 nm nanodot. In addition, it is shown that the hysteresis of the loop as well as the maximum strain value become larger with temperature decreasing. The strain becomes larger because the polarization becomes larger at lower temperatures as determined by the Landau free energy shown in Eq. (2). On the other hand, the hysteresis becomes larger because the energy barrier between different polarization variants becomes larger when temperature decreases which can also be deduced from the Landau free energy and thus larger electric fields are needed to trigger polarization switching.

3.3. Origin of the recoverable electrostrain at ferroelectric nanodots

To explore the origin of the recoverability of the vortex structure and the electrostrain of the D=40 nm nanodot, we first analyze how the vortex structure returns to its original state upon increasing and decreasing the electric field. Fig. 4 gives the domain structure evolution upon increasing and decreasing the electric fields at two temperatures

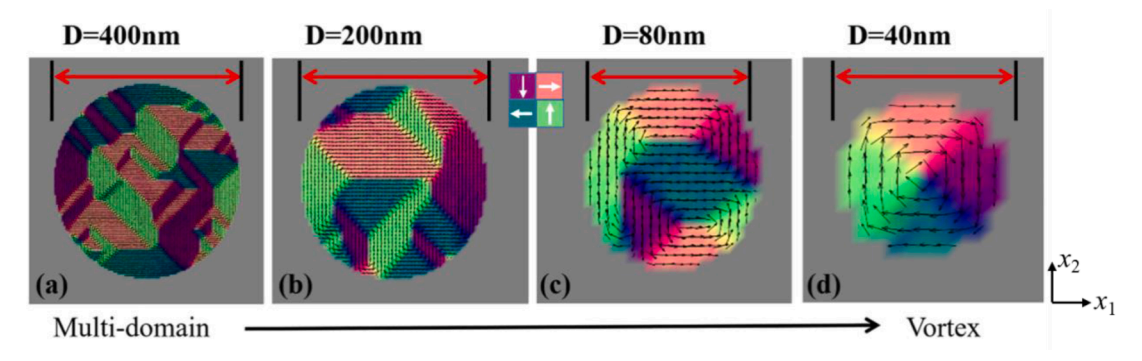


Fig. 1. Change of domain structure with the dimension of ferroelectric dots at 40°C. Arrows and colors describe the four different polarization directions respectively.

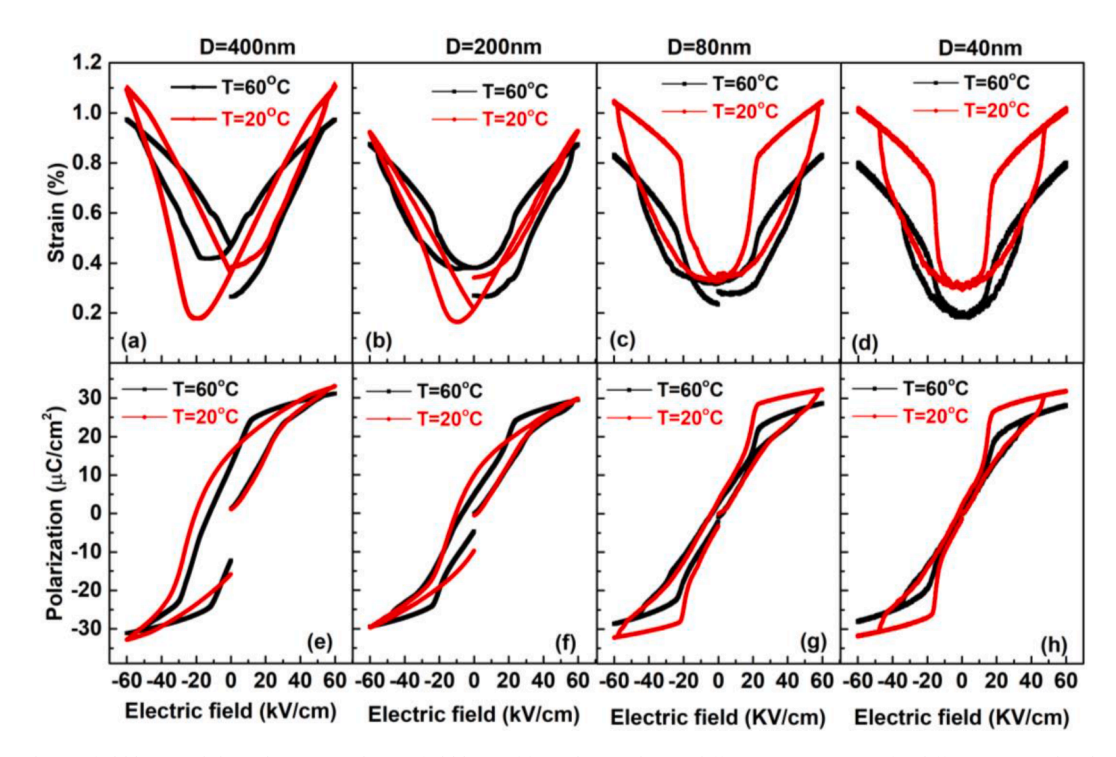


Fig. 2. The strain-electric field loop and the polarization-electric field loop of ferroelectric dots at different temperatures for different sizes. The electric field is along x_1 direction. The polarization and strain on x_1 direction are recorded.

(T=60 °C and 20 °C). It is seen that at both temperatures, upon increasing the electric field, the vortex gradually evolves into a singledomain state through domain wall motion. Interestingly, upon decreasing the electric field, the single domain reverts back to the vortex structure through nucleation and growth process, and it is seen that the nucleation always starts from the surface as found for surface chargeinduced polarization switching in PbZr_{0.2}Ti_{0.8}O₃ BiFeO3 thin films [37]. Such phenomenon can be attributed to the surface effect because at the surface of the single domain state, the polarization gradient is large, and the minimization of gradient energy in Eq. (1) would tend to align the polarization at the surface parallel to it, i.e., $\nabla P \approx 0$ [33]. More importantly, the minimization of the electrostatic energy would tend to align the new polarizations formed at the surface into flux-closure configuration. Therefore, the flux-closure loop firstly forms around the surface of the nanodot and then gradually spreads into the inside with further decrease of the electric field. As the external electric field finally decreases to zero, the vortex structure forms. Note that the recovered vortex after electric field cycling may switch to "anticlockwise-vortex" from the initial "clockwise-vortex" as shown in Fig. 4(a). This is because both vortex structures possess identical free energy and which vortex

would appear depends on the random nucleation at the surface here. Note that the chirality of the vortex can be also manipulated by local surface charge or electric field as reported in Ref. [38].

On the other hand, at larger dot sizes (e.g., R = 200 nm or 400 nm), with the removal of the external electric field, although nucleation of new polarizations occurs at the surface of the single-domain structure and grows into the inside similarly, the polarization remains unchanged at the center of the dots. Fig. 5 illustrates the domain structure evolution under external electric fields at ferroelectric nanodots with different sizes. It is demonstrated clearly that with the increase of electric field, all systems transform from multidomain/vortex structure to single-domain structure. However, with the removal of the electric field, ferroelectric nanodots with small sizes (e.g., R = 40 nm) could transform back to the vortex structure while ferroelectric nanodots with larger sizes (e.g., R =200 nm or R = 400 nm) would only transform into a near single-domain structure with the center of the dot keeping the polarization the same as that of the single domain at large fields. To understand such differences, the energy density of different polarization structures appearing upon removing the electric field for dots with different sizes(D=40 nm, D=200 nm, and D=400 nm) is calculated and the results are shown in

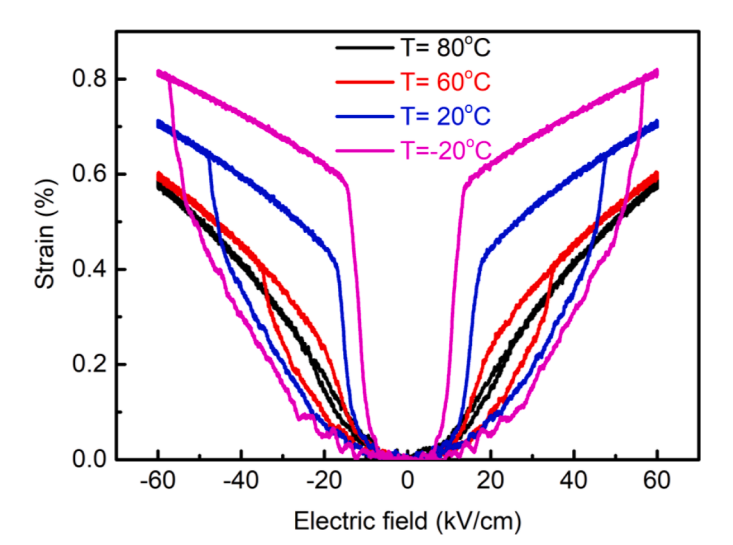


Fig. 3. The strain-electric field loop of D=40nm ferroelectric nanodots at different temperatures.

Fig. 6. It is illustrated that as the size of the dots decreases, the energy barrier between the single-domain structure and the multi-domain structure (for D=200 nm and 400 nm dots) or vortex structure (for D=40 nm dots) becomes gradually reducing. The decreasing energy barrier between the single-domain structure and the vortex/multidomain structure with reduced dot sizes could help explain why the vortex structure of the nanodots is easier to recover itself than the multi-domain structure and the vortex structure transform to single-domain structure at large electric fields.

Further simulations turning off one of the energy terms each time have confirmed that the electrostatic energy along with the elastic energy plays the main role in the recoverability of the vortex structure. Fig. 7 demonstrates the S-E loops and the polarization state upon removal of electric field for D=40nm nanodot at $T=60\,^{\circ}\mathrm{C}$ and $T=20\,^{\circ}\mathrm{C}$ for five cases: case 1(with all the energy terms on); case 2(with the depolarization field turned off), case 3(with the elastic constraint turned

off); case 4(with the elastic interaction turned off); case 5(with the dipole-dipole interaction turned off). It is illustrated from Fig. 7 that when the depolarization field is turned off (case 2), the recoverability of the S-E loop maintains at both two temperatures. On the other hand, when the elastic constraint is turned off (case 3), the recoverability of S-E loop becomes limited, especially at low temperature (20 $^{\circ}$ C). The domain pattern shown in Fig. 7(h) demonstrates that at case 3, the fluxclosure domain pattern is partially reserved and the volume fractions of different polarization directions are not all equal at the low temperature. Furthermore, when the elastic interaction is turned off (case 4), the recoverability of the S-E loop becomes more limited, especially at the low temperature (20 $^{\circ}$ C). The domain pattern shown in Fig. 7(d) and 7(i) demonstrates that at case 4, at the high temperature (60 $^{\circ}\text{C})$ the volume fractions of different polarization directions are not equal although fluxclosure domain pattern is reserved and at the low temperature (20 °C), the flux-closure domain pattern is almost lost and the nanodot is filled with polarizations aligned along the field direction. Finally, when the dipole-dipole interaction is turned off (case 5), the S-E loops at both temperatures completely lose the recoverability, and with the removal of the electric field, the nanodot maintains the single-domain state. Therefore, it is illustrated that the dipole-dipole interaction plays a major role in regulating the vortex structure and the recoverability of S-E loop. The elastic interaction (including elastic constraint) also contributes to the recoverability of vortex domain structure and S-E loop but the contribution is not as significant as the dipole-dipole interaction.

3.4. Polar vortex structure and recoverable electrostrain obtained in a 3-dimensional (3D) ferroelectric nanodot

The above simulations are performed in 2-dimensional (2D). To verify that the electrostrain of polar vortex structure is also recoverable in 3-dimensional (3D) cases, phase field simulations on a 3D ferroelectric nanodot are also performed. Fig. 8(a) shows the polar vortex structure obtained in a 3D nanodot with D= 40 nm at T=40 °C. It is illustrated that the vortex forms in the x_1 - x_3 plane. Fig. 8(b) shows the P-E and S-E loop of this nanodot (the external field direction is along x_1 direction). Clearly, the polarization and electrostrain are both recoverable. Fig. 8(c) then gives the change of the polar structure of this nanodot upon increasing and decreasing the electric field, which

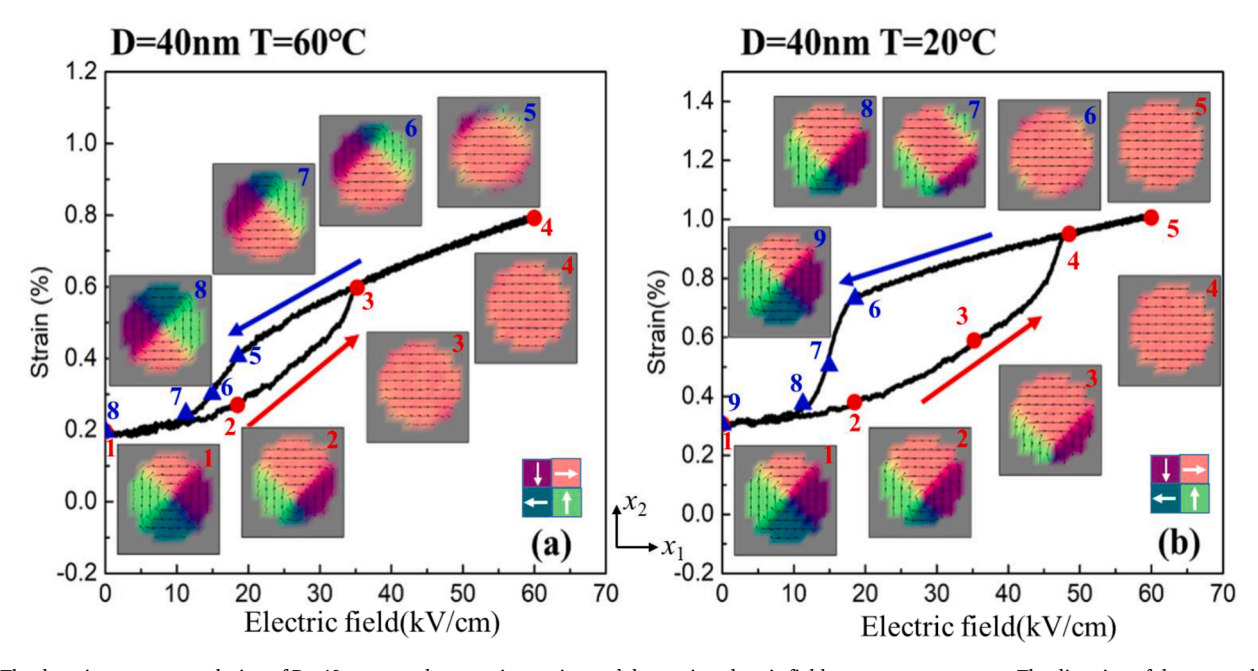


Fig. 4. The domain structure evolution of D=40 nm nanodot upon increasing and decreasing electric fields at two temperatures. The direction of the external electric field is along x_1 direction. The colors in the domain structure represent different polarization directions.

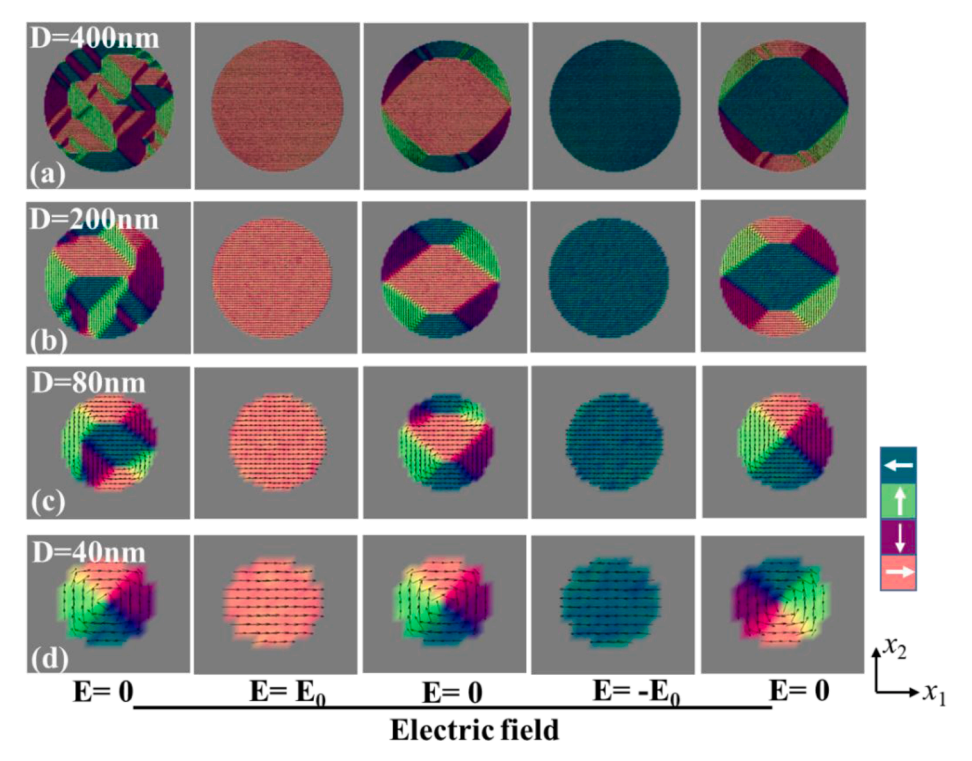


Fig. 5. Domain structure evolution under electrical fields for ferroelectric nanodots with different sizes. (a) D=400 nm, (b) D=200 nm, (c) D=80 nm, (d) D=40 nm. Arrows and colors describe the four different polarization direction respectively. The electric field is along x_1 direction.

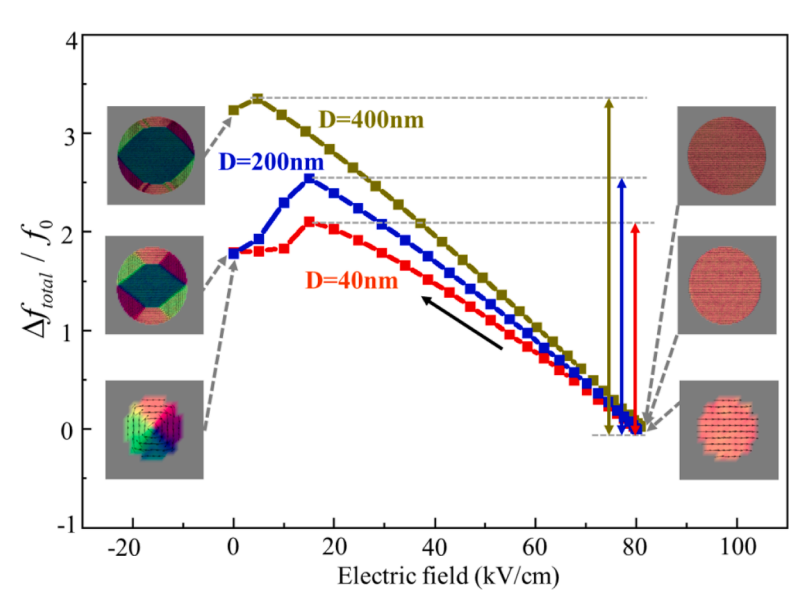


Fig. 6. Variation of the reduced total energy density of different polarization structures appearing upon removing external electric fields for dots with different sizes(D=40nm, 200nm and 400nm). The energy barrier between the single-domain structure and multi-domain/vortex structure for different dot sizes is indicated by the double-headed arrows. $\triangle f_{\text{total}}$ is the difference of the total energy density between the polarization structures at different electric fields of each dot and its single-domain structure at 80kV/cm, f_0 is a normalization constant.

illustrate that similar mechanism as that for the 2D nanodots (as shown in Fig. 4) operates in the recoverability of the electrostrain. Note that upon removing electric fields the vortex forms in the x_1 - x_2 plane rather than in the initial x_1 - x_3 plane due to the random nucleation at the surface, which is similar to the case shown in Fig. 4(a) obtained for the 2D nanodots.

3.5. Comparison with recoverable electrostrain obtained in bulk ferroelectrics

In bulk ferroelectrics, there are two common ways to recover the initial multidomain state and obtain recoverable electrostrain. One is utilizing the large local electric fields induced by point defects (i.e., in

relaxor ferroelectrics) [13–16], and the other is utilizing the restoring force provided by the reorientable defect dipoles (i.e., in aged acceptor-doped ferroelectrics) [12]. However, the recoverable electrostrain of relaxor ferroelectrics suffers from temperature instability and the strain magnitude is not large as a result of the large number of point defects in it [13,15,16]. On the other hand, the stability of the recoverable electrostrain in aged acceptor-doped ferroelectrics is also limited because the ageing state of it could easily be destroyed by temperature increasing [12]. Therefore, the recoverable electrostrains obtained in bulk ferroelectrics are limited for real applications on actuators. In contrast, the recoverable electrostrain achieved in ferroelectric nanodots has the following two advantages: (1) The strain value maintains a large value; (2) the temperature stability is good. These two

X. Ke et al. Acta Materialia 250 (2023) 118866

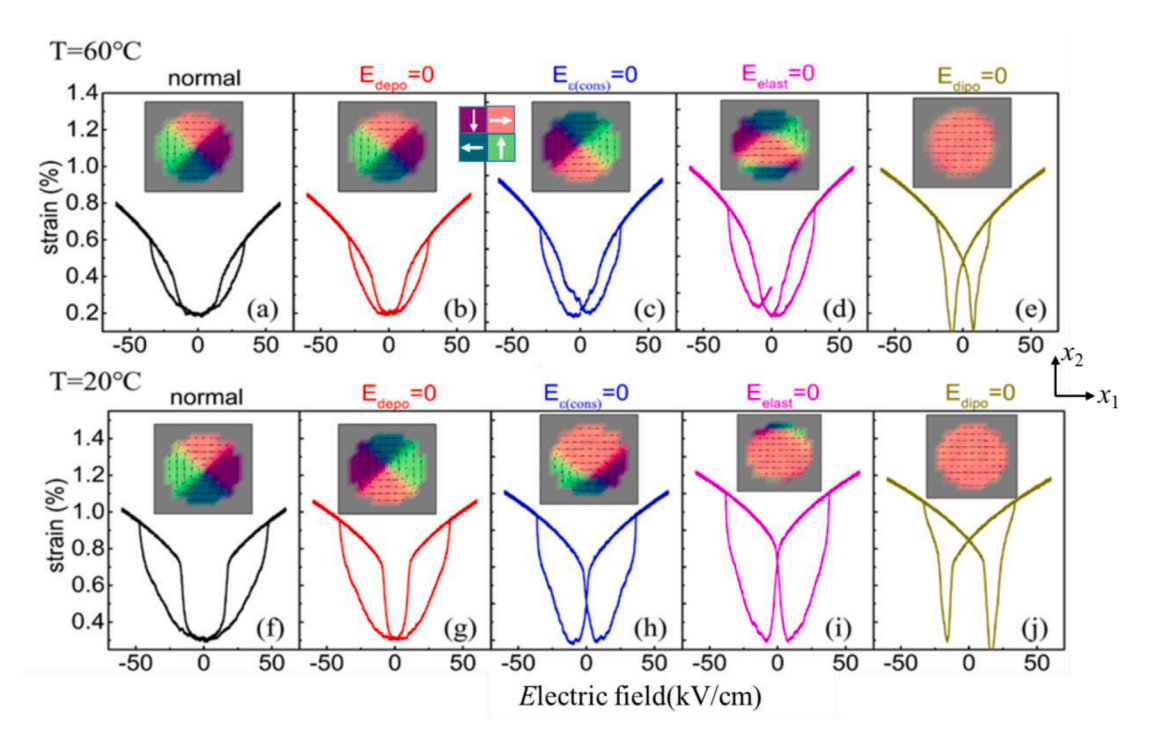


Fig. 7. Effect of depolarization energy, elastic constraint, elastic energy and electrostatic energy on the recoverability of vortex domain structure and S-E loop of D=40nm nanodot at two temperatures at five cases: (a) and (f) case 1 (all energy terms are turned on). (b) and (g) case 2(the depolarization energy term is turned off). (c) and (h) case 3(the elastic constraint is turned off). (d) and (i) case 4(the elastic interaction is turned off). (e) and (j) case 5(the dipole-dipole interaction is turned off).

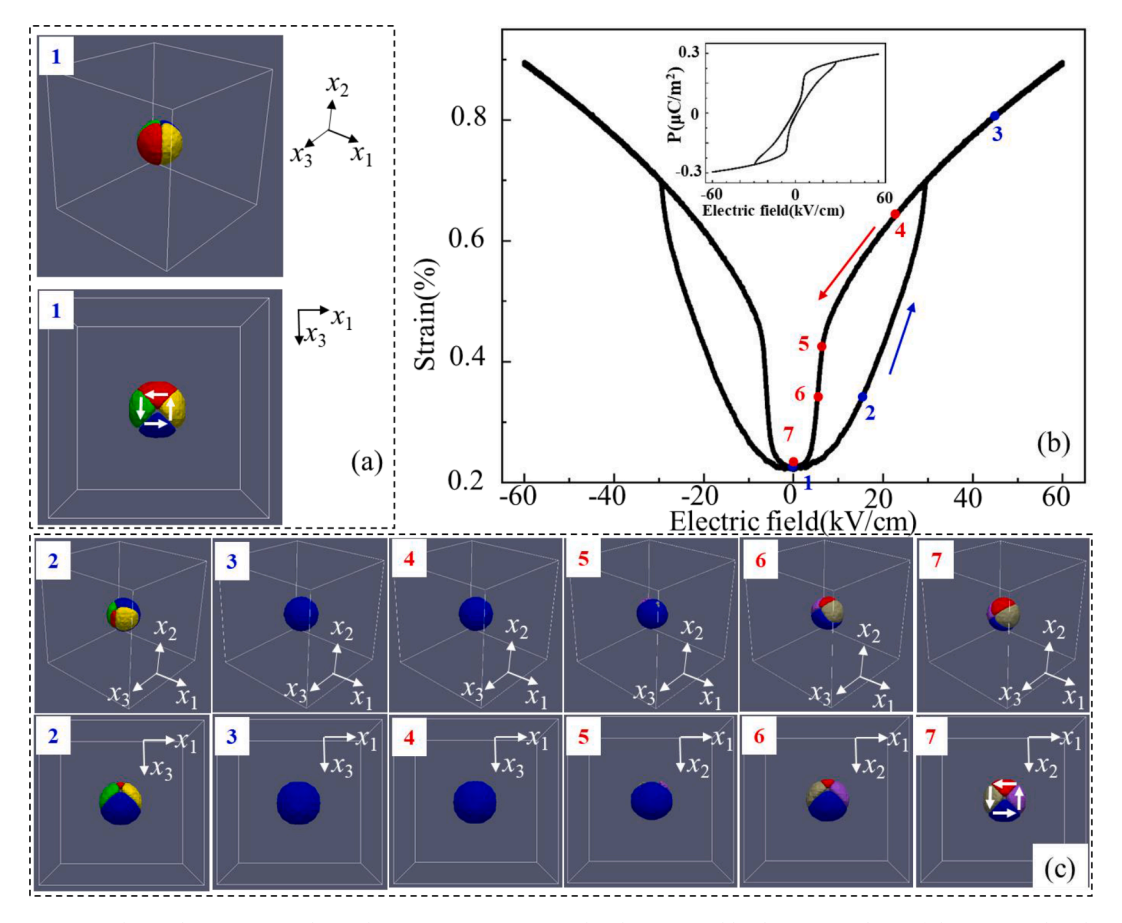


Fig. 8. (a) Vortex structure obtained in a 3D nanodot with D=40nm at T=40 $^{\circ}$ C. (b) The recoverable electrostrain loop of the 3D nanodot obtained by applying external electric fields along x_1 direction. The inset figure gives the recoverable polarization-electric field loop. (c) The evolution of the polarization structure upon increasing and decreasing the electric field of the vortex.1-7 indicate the 7 points on the recoverable electrostrain shown in Fig. 8(b).

characteristics of the recoverable electrostrain achieved in ferroelectric nanodots are beneficial for their applications in MEMS and NEMS as nanoactuators. In addition, the recoverable electrostrain achieved in ferroelectric nanodots with vortex structure should be general for any ferroelectric systems, which offers a wide range of material choices. Furthermore, unlike the recoverable electrostrain obtained for bulk ferroelectrics mentioned above, the recoverable electrostrain in ferroelectric nanodots does not rely on any point defects, which could ease the process of fabrication. Despite of all the above advantages, the recoverable vortex structure and large recoverable electrostrain appear only in ferroelectric nanodots with a narrow range of sizes as illustrated in Figs. 1 and 2, which could limit its real application.

4. Conclusions

In conclusion, we report fully recoverable vortex structure and large recoverable electrostrain over a wide temperature range in nanodots with constrained elastic boundary and open-circuit electric boundary. The recoverability of the electrostrain is due to the restoring force provided mainly by the dipole-dipole interaction energy and elastic energy. The large recoverable strain over a wide temperature range for ferroelectric nanodots does not rely on point defects and should be general for any ferroelectric systems. This work could stimulate further research on applications of ferroelectric nanodots on MEMS and NEMS.

Declaration of Competing Interest

The authors declare that they have no known competing financial interests or personal relationships that could have appeared to influence the work reported in this paper.

Acknowledgment

This work was supported by National Key R&D Program of China (2021YFB3803003), Natural Science Foundation of Ordos (Grant No. 2021EEDSCXQDFZ014), and National Natural Science Foundation of China (Grant No. 52171189, 52171012, 51931004 and No. 52171190) and 111 project (BP2018008). YW acknowledges the US Natural Science Foundation (Grant No. DMR-1923929), which has facilitated this international collaboration.

References

- J. Hlinka, P. Ondrejkovic, Skyrmions in ferroelectric materials, Solid State Phys. (2019).
- [2] S. Das, Z. Hong, M. McCarter, P. Shafer, Y.T. Shao, D.A. Muller, L.W. Martin, R. Ramesh, A new era in ferroelectrics, APL Mater. 8 (2020), 120902.
- [3] J.M. Gregg, Exotic domain states in ferroelectrics: searching for vortices and skyrmions, Ferroelectrics 433 (2012) 74.
- [4] I.I. Naumov, L. Bellaiche, H. Fu, Unusual phase transitions in ferroelectric nanodisks and nanorods, Nature 432 (2004) 737.
- [5] A. K.Yadav, C.T. Nelson, S.L. Hsu, Z. Hong, J.D. Clarkson, C.M. Schleputz, A. R. Damodaran, P. Shafer, E. Arenholz, L.R. Dedon, D. Chen, A. Vishwanath, A. M. Minor, L.Q. Chen, J.F. Scott, L.W. Martin, R. Ramesh, Observation of polar vortices in oxide superlattices, Nature 530 (2016) 198.
- [6] Y.L. Tang, Y.L. Zhu, X.L. Ma, A.Y. Borisevich, A.N. Morozovska, E.A. Eliseev, W. Y. Wang, Y.J. Wang, Y.B. Xu, Z.D. Zhang, S.J. Pennycook, Observation of a periodic array of flux-closure quadrants in strained ferroelectric PbTiO3 films, Science 348 (2015) 547.
- [7] C.L. Jia, K.W. Urban, M. Alexe, D. Hesse, I. Vrejoiu, Direct observation of continuous electric dipole rotation in flux-closure domains in ferroelectric Pb (Zr, Ti) O3, Science 331 (6023) (2011) 1420–1423.
- [8] N. Balke, B. Winchester, W. Ren, Y.H. Chu, A.N. Morozovska, E.A. Eliseev, M. Huijben, R. K.Vasudevan, P. Maksymovych, J. Britson, S. Jesse, I. Kornev,

- R. Ramesh, L. Bellaiche, L.Q. Chen, S.V Kalinin, Enhanced electric conductivity at ferroelectric vortex cores in BiFeO3, Nat. Phys. 8 (1) (2012) 81–88.
- [9] D. Liu, X. Shi, J. Wang, X. Cheng, H. Huang, Phase-field simulations of surface charge-induced ferroelectric vortex, J. Phys. D Appl. Phys. 54 (2021), 405302.
- [10] K. Uchino, Ferroelectric Devices, CRC Press, 2018.
- [11] I. Naumov, H. Fu, Vortex-to-polarization phase transformation path in ferroelectric Pb(ZrTi)O3 nanoparticles, Phys. Rev. Lett. 98 (2007), 077603.
- [12] X. Ren, Large electric-field-induced strain in ferroelectric crystals by point-defectmediated reversible domain switching, Nat. Mater. 3 (2004) 91–94.
- [13] S. Semenovskaya, A.G. Khachaturyan, Development of ferroelectric mixed states in a random field of static defects, J. Appl. Phys. 83 (1998) 5125.
- [14] X. Shi, J. Wang, J. Xu, X. Cheng, H. Huang, Quantitative investigation of polar nanoregion size effects in relaxor ferroelectrics, ACTA Mater. 237 (2022), 118147.
- [15] Z. Hong, X. Ke, D. Wang, S. Yang, X. Ren, Y. Wang, Role of point defects in the formation of relaxor ferroelectrics, Acta Mater. 225 (2022), 117558.
- [16] S.-T. Zhang, A.B. Kounga, E. Aulbach, H. Ehrenberg, J. Rodel, Giant Strain in lead-free piezoceramics Bi_{0.5}Na_{0.5}TiO₃-BaTiO₃-K_{0.5}Na_{0.5}NbO₃ system, Appl. Phys. Lett. 91 (2007), 112906.
- [17] S.E. Lyshevski, MEMS and NEMS: Systems, Devices, and Structures, CRC press,
- [18] D. Pappas, Z.G. Fthenakis, I. Ponomareva, All-mechanical polarization control and anomalous (electro) mechanical responses in ferroelectric nanowires, Nano Lett. 18 (9) (2018) 5996–6001.
- [19] X. Fu, I.I. Naumov, H. Fu, Collective dipole behavior and unusual morphotropic phase boundary in ferroelectric Pb(Zr0.5Ti0.5)O3 nanowires, Nano Lett. 13 (2) (2013) 491–496.
- [20] Y. Ji, W.J. Chen, Y. Zheng, Crossover of polar and toroidal orders in ferroelectric nanodots with a morphotropic phase boundary and nonvolatile polar-vortex transformations, Phys. Rev. B 100 (1) (2019), 014101.
- [21] B. Lee, S.M. Nakhmanson, O. Heinonen, Strain induced vortex-to-uniform polarization transitions in soft-ferroelectric nanoparticles, Appl. Phys. Lett. 104 (26) (2014), 262906.
- [22] W.J. Chen, Y. Zhang, B. Wang, Large and tunable polar-toroidal coupling in ferroelectric composite nanowires toward superior electromechanical responses, Sci. Rep. 5 (2015) 11165.
- [23] S. Choudhury, Y.L. Li, C.E. Krill Iii, L.Q. Chen, Phase-field simulation of polarization switching and domain evolution in ferroelectric polycrystals, Acta Mater. 53 (20) (2005) 5313–5321.
- [24] J.J. Wang, B. Wang, L.Q. Chen, Understanding, predicting, and designing ferroelectric domain structures and switching guided by the phase-field method, Annu. Rev. Mater. Res. 49 (2019) 127–152.
- [25] C. Shen, J.P. Simmons, Y. Wang, Effect of elastic interaction on nucleation: II. Implementation of strain energy of nucleus formation in the phase field method, Acta Mater 55 (2007) 1457.
- [26] D. Wang, X. Ke, Y. Wang, J. Gao, Y. Wang, L. Zhang, S. Yang, X. Ren, Phase diagram of polar states in doped ferroelectric systems, Phys. Rev. B 86 (2012), 054120.
- [27] J. Wang, & M. Kamlah, Domain control in ferroelectric nanodots through surface charges, Appl. Phys. Lett. 93 (26) (2008), 262904.
- [28] J. Wang, & M. Kamlah, Domain structures of ferroelectric nanotubes controlled by surface charge compensation, Appl. Phys. Lett. 93 (4) (2008), 042906.
- [29] I. Ponomareva, I.I. Naumov, L. Bellaiche, Low-dimensional ferroelectrics under different electrical and mechanical boundary conditions: Atomistic simulations, Phys. Rev. B 72 (21) (2005), 214118.
- [30] A. Schilling, D. Byrne, G. Catalan, K.G. Webber, Y.A. Genenko, G.S. Wu, J. M. Gregg, Domains in ferroelectric nanodots, Nano Lett. 9 (9) (2009) 3359–3364.
- [31] B.J. Rodriguez, X.S. Gao, L.F. Liu, W. Lee, I.I. Naumov, A.M. Bratkovsky, D. Hesse, M. Alexe, Vortex polarization states in nanoscale ferroelectric arrays, Nano Lett. 9 (3) (2009) 1127–1131.
- [32] L.L. Ding, Y. Ji, X.Y. Zhang, W.M. Xiong, W.J. Chen, B.M. Zhang, Y. Zheng, Characterization and control of vortex and antivortex domain defects in quadrilateral ferroelectric nanodots, Phys. Rev. Mater. 3 (10) (2019), 104417.
- [33] H. Fu, L. Bellaiche, Ferroelectricity in barium titanate quantum dots and wires, Phys. Rev. Lett. 91 (2003), 257601.
- [34] J. Slutsker, A. Artemev, A. Roytburd, Phase-field modeling of domain structure of confined nanoferroelectrics, Phys. Rev. Lett. 100 (8) (2008), 087602.
- [35] J. Wang, Switching mechanism of polarization vortex in single-crystal ferroelectric nanodots, Appl. Phys. Lett. 97 (19) (2010), 192901.
- [36] D. Karpov, Z. Liu, T. Rolo, R. Harder, P.V. Balachandran, D. Xue, T. Lookman, E. Fohtung, Three-dimensional imaging of vortex structure in a ferroelectric nanoparticle driven by an electric field, Nat. Commun. 8 (1) (2017) 1–8.
- [37] D. Liu, R. Zhao, H.M. Jafri, J. Wang, H. Huang, Phase-field simulations of surface charge-induced polarization switching, Appl. Phys. Lett. 114 (2019), 112903.
- [38] D. Liu, J. Wang, H.M. Jafri, X. Wang, X. Shi, D. Liang, C. Yang, X. Cheng, H. Huang, Phase-field simulations of vortex chirality manipulation in ferroelectric thin films, npj Quantum Mater. 7 (1) (2022) 1–8.